

RESEARCH PAPER



MiR-125-5p/IL-6R axis regulates macrophage inflammatory response and intestinal epithelial cell apoptosis in ulcerative colitis through JAK1/STAT3 and NF- κ B pathway

Danhua Yao*, Zhiyuan Zhou*, Pengfei Wang, Lei Zheng, Yuhua Huang, Yantao Duan, Bin Liu, and Yousheng Li

Department of General Surgery, Shanghai Ninth People's Hospital, Shanghai JiaoTong University School of Medicine, Shanghai, China

ABSTRACT

This study explored the effects of miR-125-5p and interleukin-6 receptor (IL-6 R) on ulcerative colitis (UC) cell models and mouse models. The sera derived from UC patients and healthy subjects were collected for expression analysis. UC *in vitro* models and *in vivo* model were constructed and used. Expressions of miR-125-5p, IL-6 R, AK1/STAT3 and NF- κ B pathways, and inflammatory factors, histopathology and apoptosis were determined by conducting a series of molecular experiments. The relationship between miR-125-5p and IL-6 R was analyzed by TargetScan7.2 and verified by dual-luciferase assay. The disease activity index (DAI) score, weight change, and colon length of the mice were recorded and analyzed. Decreased expression of miR-125-5p in the sera of UC patients was related to the increased expression of its target gene IL-6 R. *In vitro*, up-regulation of miR-125-5p decreased IL-6 R expression, contents of inflammatory factors in THP-1 cells and cell apoptosis of NCM460, and inhibited the activation of JAK1/STAT3 and NF- κ B pathway. However, down-regulation of miR-125-5p produced the opposite effects to its up-regulation. IL-6 R overexpression partially reversed the effects of miR-125-5p up-regulation on UC cell models. *In vivo*, miR-125-5p overexpression significantly improved the severity of colitis, including DAI score, colon length, tissue damage, apoptosis, and inflammatory response, in the mice in the UC group. In addition, miR-125-5p up-regulation significantly reduced the expression of IL-6 R in the UC mice, and reduced the expression levels of JAK1, STAT3 and p65 phosphorylation. MiR-125-5p targeting IL-6 R regulates macrophage inflammatory response and intestinal epithelial cell apoptosis in ulcerative colitis through JAK1/STAT3 and NF- κ B pathway.

ARTICLE HISTORY

Received 3 June 2020
Revised 10 August 2021
Accepted 13 October 2021



KEYWORDS

Ulcerative colitis; MiR-125-5p; interleukin 6 receptor; inflammatory; apoptosis

Introduction

Ulcerative colitis (UC) is a nonspecific colonic inflammation, and both UC and Crohn's disease are inflammatory bowel diseases (IBDs) [1]. UC, which mainly occurs at the colonic mucosa or submucosa, can lead to excessive immune response in the human body, resulting in the production of a large number of inflammatory cytokines and induction of apoptosis of intestinal epithelial cells [2]. UC is clinically manifested as rectal bleeding and severe diarrhea [3]. The treatment of UC imposes great difficulties and its incidence is increasing annually [4]. As the pathogenesis and pathogenic factors of UC are still unclear, it is particularly urgent to study the pathogenesis of UC for developing an effective method to treat UC.

MiRNAs has become biomarkers and potential therapeutic targets in disease diagnosis and treatment [5,6]. It is now widely acknowledged that miRNAs play important roles in the pathogenesis of intestinal diseases, particularly, differentially expressed miRNAs have been proven to have critical functions in the colon mucosa, as they can maintain intestinal mucosal immunity and intestinal barrier permeability integrity [7–10]. He et al. found that miR-301A expression is elevated in patients with active IBD, and miR-301A can reduce the expression of BTG1 and the integrity of mouse colon epithelium, promote inflammatory response, thereby contributing to tumorigenesis [11]. Moreover, miR-320a has been found to inhibit the damage of E. coli-induced to the function of intestinal barriers, and its level is increased in

CONTACT Yousheng Li  liyoushengly@163.com  Department of General Surgery, Shanghai Ninth People's Hospital, Shanghai JiaoTong University School of Medicine, No. 639 Zhizaoju Road, Shanghai, China

*These authors contributed equally to this work.

© 2021 Informa UK Limited, trading as Taylor & Francis Group

blood samples derived from UC mice [12]. A previous study demonstrated that overexpression of miR-125 reduces STAT3 phosphorylation in human intestinal epithelial cells [13]. However, the understanding of the regulation, biological effects, and targets of miR-125-5p in UC is currently limited.

The expression and regulation of interleukin (IL) 6 and IL6 receptor (IL-6 R) are related to the occurrence and development of many tumors [14,15]. At present, abnormal expressions of IL-6 and IL-6 R have been found in tumor tissues of kidney cancer, prostate cancer, liver cancer, and esophageal cancer [16,17]. Studies also uncovered that the expressions of IL-6 and IL-6 R are significantly up-regulated in UC patients [18]. IL6, a typical pro-inflammatory factor, contributes to the development of UC through the membrane-bound IL-6 R [19]. Some researchers observed that miR-21-5p can mediate UC through the IL-6 R/STAT3 pathway [20], but whether miR-125-5p also regulated the role of IL-6 R in UC remained to be determined.

In the current study, based on the study of Manying Li et al [21], we used lipopolysaccharide (LPS)-induced acute conjunctivitis cell model and established a UC mouse model by dextran sodium sulfate (DSS) treatment, so as to explore the roles of miR-125-5p and IL-6 R in the development of UC. The aim of this research was to provide a research basis for the development of a possible therapeutic target and molecular basis.

Materials and methods

Ethics statement

Both clinical and animal studies were approved by the Ethics Committee of Shanghai Ninth People's Hospital, Shanghai JiaoTong University School of Medicine (XH201712031) and the Institutional Animal Care and Use Committee of Shanghai Ninth People's Hospital, Shanghai JiaoTong University School of Medicine (D201907011). All the subjects were fully informed of the whole study. All animal studies were conducted following the regulations of standard animal care and laboratory guidelines.

Sera specimens, cell and culture

The sera in this study were collected from 20 active UC patients who received colonoscopy and from 19 healthy subjects at our hospital between January 2018 and December 2019. The patients were all pathologically confirmed as having UC. The serum specimens were obtained from the UC patients and healthy subjects, and quickly stored at -80°C . Patients confirmed as having UC were included. Healthy subjects without other illness confirmed by a medical examination were enrolled as healthy controls. Patients with polar outbreak type and chronic persistent type of UC, with more severe illness, infectious bowel disease or Crohn's disease, ischemic bowel disease or radiation enteritis were excluded. Moreover, subjects during pregnancy, patients with allergies, mental illnesses or other major diseases were also excluded. In addition, the included UC patients were not treated with other drugs, and their clinical manifestations were consistent. The clinical data of the patient are shown in Table 1.

THP-1 (TIB-202, American Type Culture Collection, USA) and NCM460 normal colonic epithelial cells (<http://www.jennio-bio.com/>, GuangZhou Jennio Biotech Co., Ltd, CA) were used in the current study. The cells were cultured following the requirements of the company. All the cells were cultured in RPMI-1640 Medium (30-2001, ATCC, USA) containing 10% Fetal Bovine Serum (FBS) (30-2020) in a 5% CO_2 incubator at 37°C . When the cells of third generation reached a concentration of logarithmic growth stage, they were used for follow-up study.

Co-culture and cell transfection

The co-cultivation system of THP-1 and NCM460 cells was established as previously described and

Table 1. The relationship between miR-125-5p expression and Ulcerative Colitis clinical characteristics.

Variable	n = 20	miR-125-5p expression		P value
		Low (n = 15)	High (n = 5)	
Gender				0.500
Male	10	7	3	
Female	10	8	2	
Age				0.704
≤60	12	9	3	
>60	8	6	2	

appropriately adjusted. To set up a co-culture model, NCM460 cells were cultured in a 6-well at a density of 2×10^5 cells/well for 17 to 20 days to obtain a complete monolayer and seeded in the upper Transwell chamber. THP-1 cells were cultured in a 6-well plate at a density of 1.5×10^6 cells/ well, treated by 10 ng/mL PMA and 0.3% bovine serum albumin for 48 hours (h) and seeded in the upper Transwell chamber. After confirming that THP-1 cells had differentiated into macrophages, the Transwell chamber used to culture the NCM460 cells for 17 to 20 days was placed in culture wells for culturing the macrophage-like THP-1 cells. Lipopolysaccharide (LPS) was then added into the lower chamber at a final concentration of 100 ng/ ml. The agomiR-NC, antagomiR-NC, agomiR-125-5p and antagomiR-125-5p groups were transfected into THP-1 cells before co-culture. The agomiR-125-5p/agomiR-NC and IL-6 R/NC overexpression plasmids were co-transfected into THP-1 cells 48 h after co-transfection, and then further co-cultured. Finally, the two cell lines were co-cultured for 24 h. All the plasmids were constructed by outsourcing of Genepharma Co., Ltd. (Shanghai, CA). In addition, the cells were transfected according to the instructions of Lipofectamine 3000 (L3000015, ThermoFisher, USA).

Real-time quantitative PCR (qRT-PCR)

Real-time quantitative PCR was performed to detect gene expression, with β -actin and U6 as internal controls. The relative expression of the target gene was calculated using the $2^{-\Delta\Delta C_t}$ method [22]. All primer sequences were shown in Table 2. In short, the total RNAs of each test sample were extracted. The specific procedures were conducted strictly by referring to the instructions of TRIzol Reagent (15,596,026, Thermo Fisher, USA). Then, the total RNA of each sample was subjected to

quantitative analysis, and the same amount of RNA was from each group was used for performing reverse transcription (One-Step PrimeScript RT-PCR Kit, RR064A, Japan). The conditions were described as follows: pre-denaturation at 95°C for 10 min, denaturation at 95°C for 15 s, annealing at 60°C for 1 min, for a total of 40 cycles. After amplified by PCR, each detection sample was quantified using a real-time quantitative PCR kit (A46113, Applied Biosystems, USA). Each sample was set up with additional 3 parallel samples and the experiment was operated in triplicate.

Bioinformatics prediction

TargetScan 7.2 (http://www.targetscan.org/vert_72/) was used to predict the binding site of miR-125-5p and IL-6 R.

Dual-luciferase activity assay

The IL-6 R fragment was inserted into the pmirGLO vector (E1330, Promega, CA, USA) as a wild-type IL-6 R plasmid (IL-6 R-WT), and the mutated binding site of IL-6 R fragment was inserted into the pmirGLO vector as a mutant IL-6 R plasmid (IL-6 R-MUT). The HEK293T cells were simultaneously transfected with agomiR-125-5p and IL-6 R-WT or IL-6 R-MUT. 48 h after the transfection, dual-luciferase reaction intensity of each group of cells was measured using a kit (FR201-01, TransGen Biotech, CA).

Enzyme-linked immunosorbent assay (ELISA)

Cell supernatants or mouse colon tissue homogenates were collected from each group. ELISA was performed to detect the expressions of interleukin-6 (IL-6, PI330-human/PI326-mouse), IL-1 β

Table 2. All primer in this study.

ID	Forward sequence(5' -3')	Reverse sequence(5' -3')
IL-6 R	CATTGCCATTGTTCTGAGGTTTC	AGTAGTCTGTATTGCTGATGTC
β -actin	GTTGGCGCCCCAGGCACCA	CTCCTTAATGTCACGCACGATTT
miR-125-5p	TGTGAGTCGTATCCAGTGCAA	GTATCCAGTGCGGTTCGTGG
U6	AGCCCGCACTCAGAACATC	GCCACCAAGACAATCATCC
IL-6 R-m	GCCACCGTTACCCTGATTTG	TCCTGTGGTAGTCCATTCTCTG
β -actin-m	GTCACGTTGACATCCGTAAAGA	GCCGGACTCATCGTACTCC

(PI305-human/PI301-mouse), and tumor necrosis factor α (TNF- α , PT518-human/PT512-mouse) in each test samples. Briefly, the supernatant was centrifuged to remove the precipitate, then added to the coated antibody microwells, and diluted. A horseradish peroxidase-labeled detection antibody was added to the supernatant for further incubation at room temperature for 20 min in the dark. After washing, the substrate was added and incubated in the dark at room temperature for another 20 min. The reaction was terminated by adding stop solution, and the OD value of each well was measured at 450 nm using a microplate reader (GX71, Olympus, Japan). The specific operation was based on the ELISA kit instructions. All the kits were purchased from Beyotime.

Flow cytometry

The cells of each group were digested by 0.25% trypsin, and the cells were collected and washed 3 times with pre-cold phosphate buffer. The cells were adjusted to a density of 1×10^4 cells/ml by binding buffer, 100 μ l of the cell suspension was added to the test tube, and then 5 μ l of Annexin V and 10 μ l of PI (APOAF, Sigma, Germany) were supplemented to the cells and incubated together for 15 min in the dark. Flow cytometry (FACScan, BD Biosciences, USA) and flow Jo V10 software (BD Biosciences) were used for the detection and analysis of cell apoptosis in each group.

Western blot analysis

Changes in related protein expressions were determined by Western blot. The specific operation began with total protein extraction, SDS-PAGE gel preparation, followed by protein loading, separation electrophoresis, and membrane transfer. Subsequently, primary antibody incubation and secondary antibody incubation were performed, followed by color development and photography. β -actin was used as a reference protein. Protein expressions were analyzed using a gel imaging system. RIPA lysate (P0013, Beyotime, CA), PVDF membrane (Immobilon-P Transfer Membrane, EMD Millipore Corporation, MA), ECL kit (SL1350-100 ml, Coolaber, China), and ImageJ (version 5.0, Bio-Rad, USA) were used in

this experiment. The primary antibodies used were as follows: IL-6 R (1/1000, sc-373,708, 80 kD, Santa Cruz), JAK1 (1/1000, ab133666, 133 kD, Abcam), p-STAT3 (1/2000, ab76315, 88 kD, Abcam), STAT3 (1/5000, ab119352, 88 kD, Abcam), p-p65 (1/2000, ab86299, 60 kD, Abcam), p65 (0.5 μ g/ml, ab16502, 64 kD, Abcam), β -actin (1 μ g/ml, ab8226, 42 kD, Abcam). Secondary antibodies were Anti-Mouse IgG (1:5000, ab205719) and Anti-Rabbit IgG (1:5000, ab205718).

Animal and modeling

To detect the effect of miR-125-5p on ulcerative colitis in vivo, we used mice to establish a disease model. 3 CRISPR-Pro-ILR6 knockout mice (weighting 18–22 g) purchased from Cyagen Biotechnology Co., LTD (China) were used to set up a UC animal model. A total of 60 C57BL/6 mice (6–8 weeks old, weighting 18–22 g) were used in this experiment. UC animal model was induced by dextran sodium sulfate (DSS). The mice were randomly divided into 6 groups ($n = 10$). All the mice except the Sham group were induced with colitis by administrating drinking water containing 5% DSS for 7 consecutive days. agomiR-125-5p, agomiR-NC, antagomiR-125-5p, and antagomiR-NC were ordered from RiboBio (Guangzhou, China). The mice in the Sham group received normal diet and saline injection; the mice in the UC group received 5% DSS drinking water for 7 consecutive days [21,23]; the mice in UC + agomiR-NC and (4) UC + agomiR-125-5p groups received were injected with 100 μ l agomiR-125-5p or agomiR-NC via tail vein 3 times a week. One week later, 5% DSS was orally administered into the mice for 7 consecutive days. agomiR-125-5p and agomiR-NC doses were used at 2 mg/ml. Changes in mouse body weight were recorded. 8 days after the colitis induction, the mice were sacrificed by cervical dislocation under anesthesia [30 mg/kg sodium pentobarbital (intraperitoneal, B5646-50 mg, ApexBio, USA)], and their colons were collected for analysis and measured for colon length. The proximal colon was cut from 10 to 15 mm, rinsed in physiological saline at 4°C, fixed by 4% paraformaldehyde, dehydrated, and then paraffin-embedded.

Disease activity index (DAI) score

The mice were scored by DAI according to the average of three parameters, which are stool consistency, stool blood and percent weight loss. The specific scoring system is as follows: weight loss percentage: 0, 1–5% = 1, 5–10% = 2, 10–20% = 3, > 20% = 4. Stool consistency: well-formed pellets = 0, soft but still-formed = 1; very soft = 2; diarrhea = 3. Fecal blood: 0 = no blood, 1 = positive blood occult blood, 2 = blood stains in the stool, 3 = major rectal bleeding.

Hematoxylin-eosin (H&E) staining

The paraffin blocks were routinely dewaxed, and then stained by hematoxylin for 7 min and by eosin for 1 min for pathological examination (H&E staining, C0105, Beyotime, CA). Morphological changes of colonic tissues of the mice were observed under eye-pieces (CKX53, OLYMPUS, Japan) after neutral gum sealing.

Transferase-mediated dUTP nick-end labeling (TUNEL) assay

To observe the apoptotic DNA fragments in the colon tissues of the mice in each group, TUNEL staining was performed according to the instructions of the kit (11,684,795,910, Roche, Switzerland). The tissue sections were routinely dehydrated and incubated with proteinase K for 15 min at 37°C. The sections were then added to the TUNEL solution and incubated for 60 min, subsequently counterstained with hematoxylin at 37°C for 5 to 30 min and then sealed. Finally, under a microscope (CKX53, OLYMPUS, Japan), 10 random areas of the sections were observed for analysis and the percentage of TUNEL positive cells was calculated.

Immunohistochemistry (IHC)

The paraffin sections of the mouse colon tissues were dewaxed, blocked by 3% H₂O₂ at room temperature, and trypsin was used for antigen retrieval. The sections were incubated with IL-6 R primary antibody (2.5 µg/ml, ab133666, Abcam) at room temperature. Next, the secondary antibody Anti-Rabbit IgG (ab205718) was added to the sections and incubated together at room temperature, rinsed in PBS,

developed by DAB solution, followed by counter-staining with hematoxylin and mounting. Each section was observed from five high-power fields under a microscope, and the expression of IL-6 R of each group was measured using Image Pro Plus 6.0 image analysis software (Media Cybernetics, USA).

Immunofluorescence

Fluorescence microscopy (BX61, Olympus, Japan) was applied to observe the transfer of P65 in mouse intestinal epithelial cell nucleus. After model building, we took tissues of model mice and fixed them in 4% formaldehyde for 24 hours. We made pathological sections (the same step as H&E staining). The tissue sections were incubated with 0.2% Triton X-100 for 10 min, then blocked the serum for 20 min at 37°C, added with the primary antibody for an overnight incubation at 4°C. Then the tissues were incubated with the secondary antibody for 1 hour at 37°C, and the nucleus was stained with DAPI (C1002, Beyotime Biotechnology, China). Next, the 100 µl stationary liquid were used to fix the tissue section. After fluorescence staining for 1 h, the fluorescence microscope is used to observe tissue sections.

Statistical analysis

The data were expressed as mean ± standard deviation (SD). Statistical analysis was performed using SPSS v18.0 software. Comparisons among multiple groups were performed using one-way analysis of variance, whereas comparisons between two groups were conducted using Student's *t*. *P* < 0.05 was defined as statistically significant. The correlation between IL-6 R and miR-125-5p was analyzed by Pearson correlation coefficient.

Results

The decreased expression of miR-125-5p in UC patients was related to the increased expression of its target gene IL-6 R

The expressions of IL-6 R and miR-125-5p were determined for the analysis of the regulatory mechanisms and physiological functions of the two in UC. As shown in Figures 1(a and b),

compared with the healthy samples, the expression of IL-6 R in the UC patients was significantly increased, while the expression of miR-125-5p was greatly decreased ($P < 0.001$). Then, the correlation between IL-6 R and miR-125-5p in UC samples was examined, and we found that the expressions of miR-125-5p and IL-6 R were significantly negatively correlated ($r = -0.575$, $p = 0.008$, Figure 1(c)). Next, we predicted and verified the targeted binding sites of miR-125-5p and IL-6 R, and found that miR-125-5p could specifically target IL-6 R ($P < 0.001$, Figure 1(d,e)).

Effect of overexpressed miR-125-5p on co-culture system of THP-1 cells and NCM460 cells in vitro

Here, as a common model to simulate UC *in vitro*, a co-culture system of THP-1 cells and NCM460

cells was used for further research [24]. The expressions of IL-6 R and miR-125-5p in the THP-1 cells were detected, and we found that agomiR-125-5p transfection can noticeably reverse the expression of miR-125-5p previously decreased by LPS, but antagomiR-125-5p further promoted the inhibitory effect of LPS on miR-125-5p expression ($P < 0.05$, Figure 2(a)). However, agomiR-125-5p transfection could greatly reverse the IL-6 R expression increased by LPS, while antagomiR-125-5p enhanced further promoted IL-6 R expression increased by LPS ($P < 0.05$, Figure 2(b-d)). ELISA was performed to further detect the effect of miR-125-5p overexpression on inflammatory factors in the co-culture system. As expected, agomiR-125-5p transfection significantly reduced the release of inflammatory factors (IL-6, IL-1 β and TNF- α) in the LPS-induced co-culture

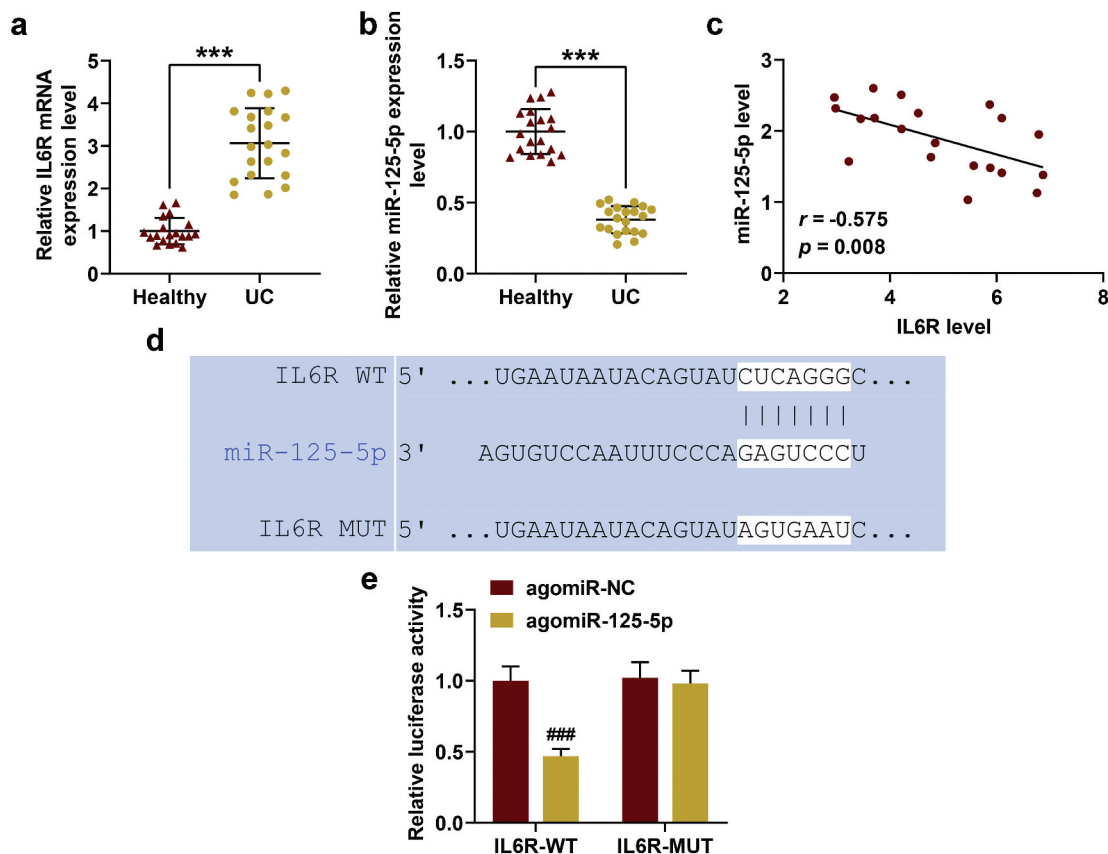


Figure 1. The decreased expression of miR-125-5p in ulcerative colitis (UC) is related to the increased expression of its target IL-6 R. (a) The expression of IL-6 R in serum specimens of healthy ($n = 19$) and UC groups ($n = 20$) was detected by reverse transcription real-time quantitative polymerase chain reaction (RT-qPCR). (b) The expression of miR-125-5p in serum specimens of healthy ($n = 19$) and UC groups ($n = 20$) was detected by RT-qPCR. (c) The correlation between IL-6 R and miR-125-5p expression in UC samples was analyzed by Pearson ($r = -0.575$, $p = 0.008$). (d) The binding site of miR-125-5p to IL-6 R was predicted using TargetScan 7.2. (e) Luciferase assay confirms the targeting relationship between miR-125-5p and IL-6 R. All experiments have been performed in triplicate. β -actin and U6 were used as controls, respectively. *** $P < 0.001$ vs. Healthy, ### $P < 0.001$ vs. agomiR-NC.

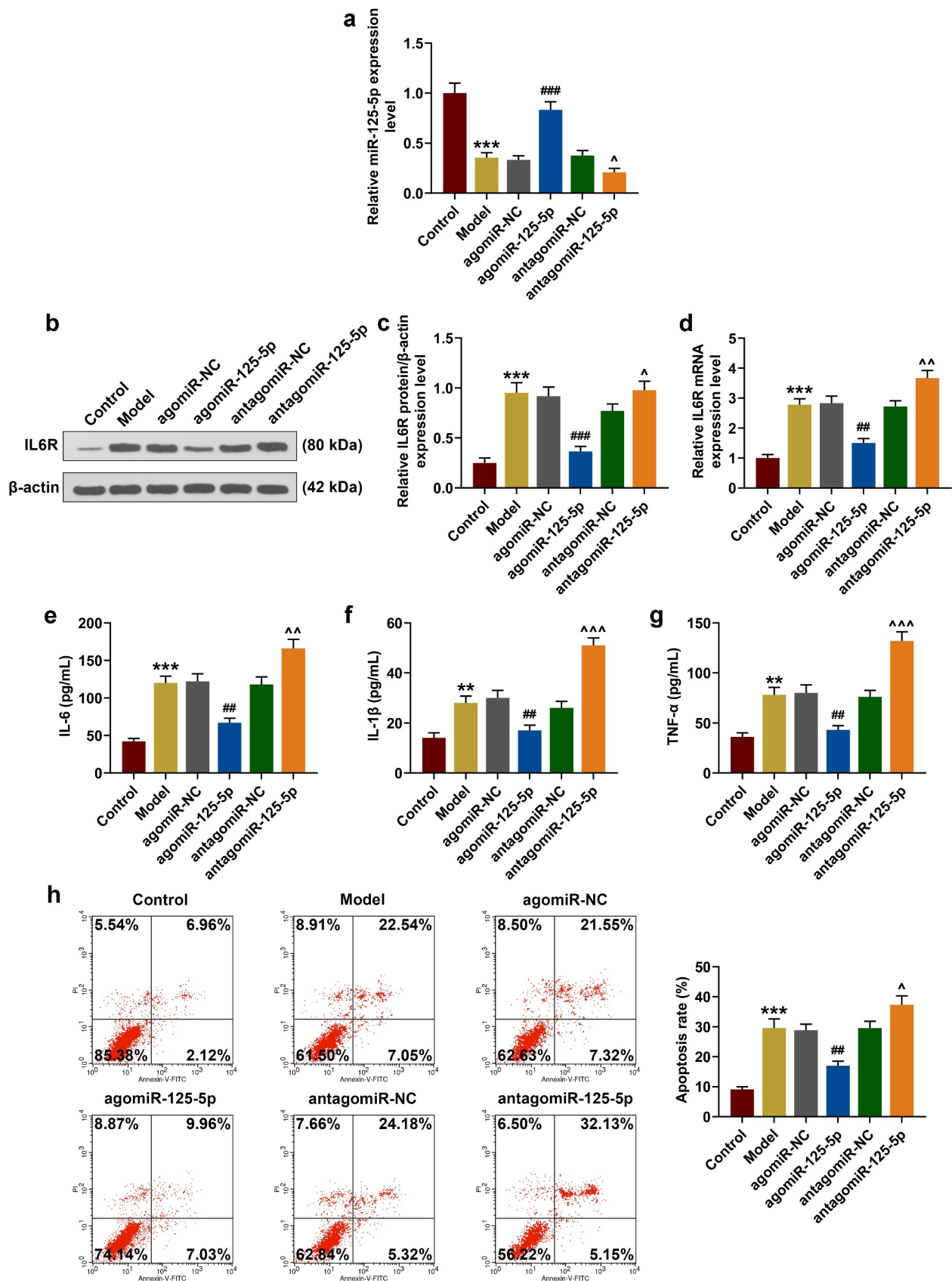


Figure 2. Effects of miR-125-5p overexpression on co-culture system of monocyte cells (THP-1) and human intestinal epithelial cells (NCM460). (a) After co-cultivation of THP-1 and NCM460 for 24 hours, the expressions of miR-125-5p in THP-1 cells of the Control, Model, agomiR-NC, agomiR-125-5p, antagomiR-NC, and antagomiR-125-5p groups were detected by reverse transcription real-time

quantitative polymerase chain reaction (RT-qPCR). (b-d) After co-culture of THP-1 and NCM460 for 24 hours, the expression of IL-6 R in THP-1 cells of each group was detected by RT-qPCR and Western blot. (e-g) Enzyme-linked immunosorbent assay (ELISA) was used to determine the contents of interleukin-6 (IL-6), IL-1 β and tumor necrosis factor- α (TNF- α) in the supernatant of medium in each group. (h) After 24-h co-culture of THP-1 and NCM460, the apoptosis of NCM460 cells was detected by flow cytometry. All the experiments have been performed in triplicate. β -actin and U6 were used as controls, respectively. ** $P < 0.01$, *** $P < 0.001$ vs. Control; ## $P < 0.01$, ### $P < 0.001$ vs. agomiR-NC; ^ $P < 0.05$, ^^ $P < 0.01$, ^^[^] $P < 0.001$ vs. antagomiR-NC.

system, while antagomiR-125-5p promoted the LPS-induced inflammatory response ($P < 0.01$, Figure 2(e-g)).

As can be seen in Figure 2(h), in the co-culture system agomiR-125-5p transfection greatly reduced NCM460 apoptosis induced by LPS, while antagomiR-125-5p promoted LPS-induced NCM460 cell apoptosis. Furthermore, as shown in Figure 3, we examined the effects of miR-125-5p on the JAK1/STAT3 signaling pathway and NF- κ B signaling pathway. Western blotting showed that the levels of JAK1, p-STAT3 and p-p65 increased significantly in the model group, while agomiR-125-5p transfection can significantly reverse the expressions of these proteins in the model group, and antagomiR-125-5p promoted the expressions of these proteins in the model group (Figure 3(a-h), $P < 0.05$), indicating that agomiR-125-5p transfection can significantly reverse the LPS-induced activation of the JAK1/STAT3 pathway in intestinal epithelial cells and at same time inhibited the activation of the NF- κ B pathway, however, antagomiR-125-5p aggravated LPS-induced activation of JAK1/STAT3 pathway and p65 phosphorylation.

IL-6 R overexpression partially reversed the effect of miR-125-5p overexpression on the co-culture system of THP-1 cells and NCM460 cells in vitro

The above studies showed that miR-125-5p overexpression played a key role in the co-culture system of THP-1 cells and NCM460 cells, therefore, the role of IL-6 R was studied by performing rescue experiment. After the transfection of IL-6 R overexpression plasmid into the cells, the transfection efficiency of IL-6 R was significantly improved in the IL-6 R group (52%) ($P < 0.05$, Figure 4(a-c)). Additionally, IL-6 R overexpression greatly enhanced the expressions of inflammatory factors, and noticeably reversed the effect of agomiR-125-5p on inhibiting THP-1 cells from releasing inflammatory factors (P

< 0.01 , Figure 4(d-f)). As shown in Figure 4(g), IL-6 R overexpression promoted apoptosis of NCM460 cells, and at the same time significantly reversed the inhibitory effect of agomiR-125-5p on the apoptosis of NCM460 cells ($P < 0.05$).

To further determine the possible molecular pathways of IL-6 R and miR-125-5p in UC, Western blot results showed that IL-6 R overexpression significantly reversed the effects of miR-125-5p overexpression on JAK1/STAT3 and NF- κ B pathways in NCM460 cells ($P < 0.05$, Figure 5(a-h)). Specifically, the expressions of JAK1, p-STAT3, and p-p65 were increased in the IL-6 R group, but decreased in the agomiR-125-5p + NC group, and were sharply lower in the agomiR-125-5p + IL-6 R group than in the IL-6 R group.

Effect of miR-125-5p agomiR on the UC mouse model in vivo

In vitro experiments showed that miR-125-5p specifically targeted IL-6 R to regulate the inflammatory response in macrophages, but reduced the apoptosis of intestinal epithelial cells. To further confirm the physiological and pathological effects of miR-125-5p *in vivo*, a UC mouse model was set up by the induction from sodium dextran sodium sulfate (DSS) in the subsequent experiments. We recorded the body weight changes of the mice in each group for 7 consecutive days, and observed that compared with the Sham group, the weight of mice in the UC group was sharply reduced during the model construction, but was greatly improved by miR-125-5p overexpression ($P < 0.001$, Figure 6(a)). As shown in Figure 6(b), the DAI score of the UC group was significantly higher than that of the Sham group, but miR-125-5p overexpression greatly lowered the DAI score of the mice in the UC group ($P < 0.001$). Importantly, the colon length in the UC group was noticeably shorter, but agomiR-125-5p injection significantly increased the length of colons in the UC group ($P < 0.01$, Figure 6(c)).

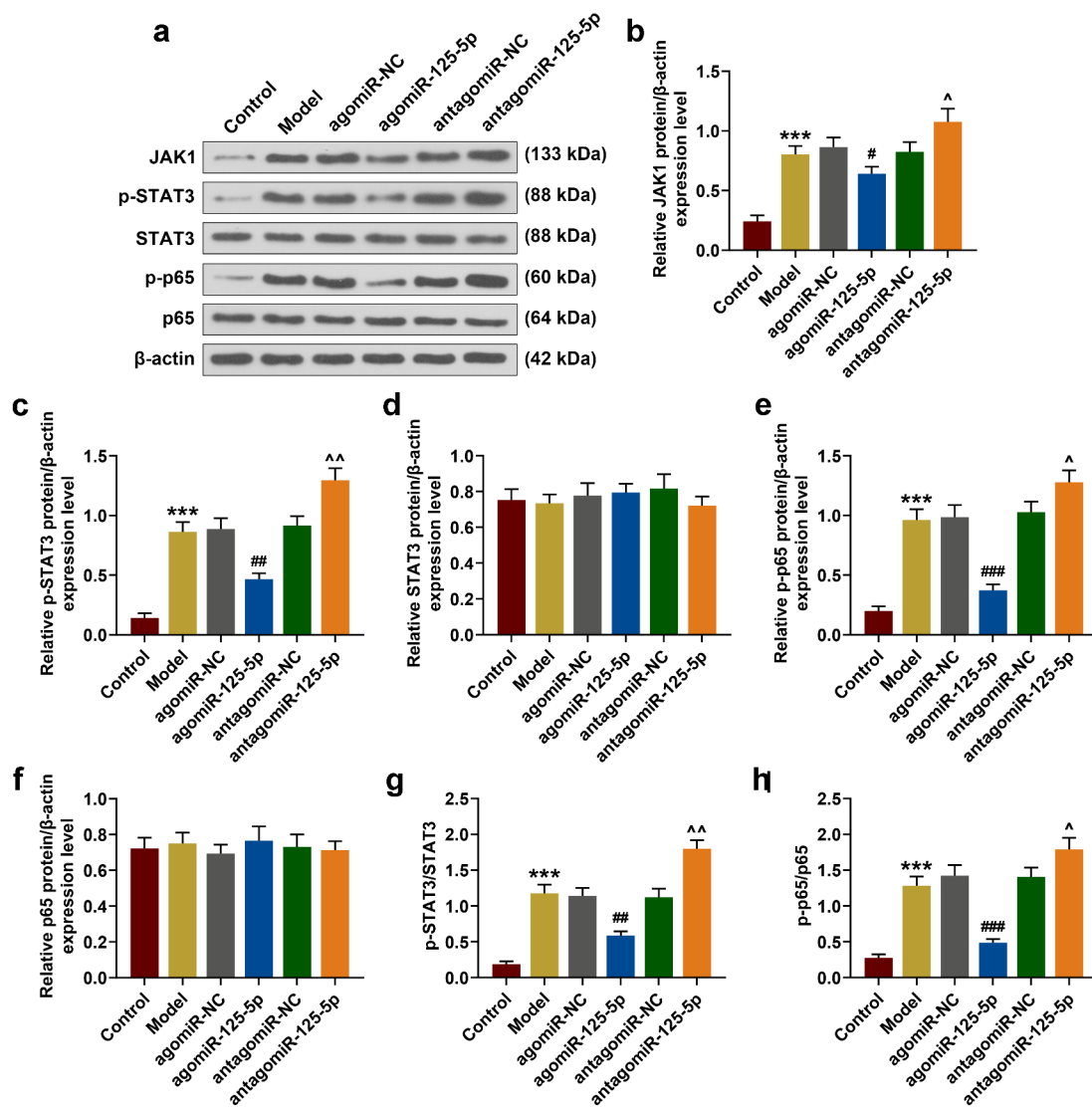


Figure 3. (a-h) Western blot was used to detect the expressions of JAK1, p-STAT3, STAT3, p-p65 and p65 in the Control, Model, agomiR-NC, agomiR-125-5p, antagomiR-NC, and antagomiR-125-5p groups. All the experiments have been performed in triplicate. β -actin was used as a control. *** $P < 0.001$ vs. Control; # $P < 0.05$, ## $P < 0.01$, ### $P < 0.001$ vs. agomiR-NC; ^ $P < 0.05$, ^^ $P < 0.01$ vs. antagomiR-NC.

The H&E staining experiment demonstrated that the colon tissue structure was complete in the Sham group, but the UC group showed crypt damage, goblet cell loss, monocyte infiltration, and severe mucosal destruction. The UC+agomiR-NC group showed diffused damage at the crypt structure, loss of goblet cells, and massive neutrophil infiltration. Meanwhile, inflammatory cell infiltration was less and the colon structure was intact without obvious ulcers in UC+agomiR-125-5p, suggesting that miR-125-5p overexpression

significantly improved colon tissue damage in the mice in the UC group (Figure 6(d)). Compared with the Sham group, the apoptosis of colon tissues of the mice in the UC group was noticeably increased, and overexpression of miR-125-5p could greatly reduce the amount of the cell apoptosis (Figure 6(e)). In addition, the contents of inflammatory factors in mouse colon tissues were significantly higher in the UC group than in the Sham group, and greatly less in the UC + agomiR-125-5p group than in the UC group ($P < 0.01$, Figure 7(a-c)).

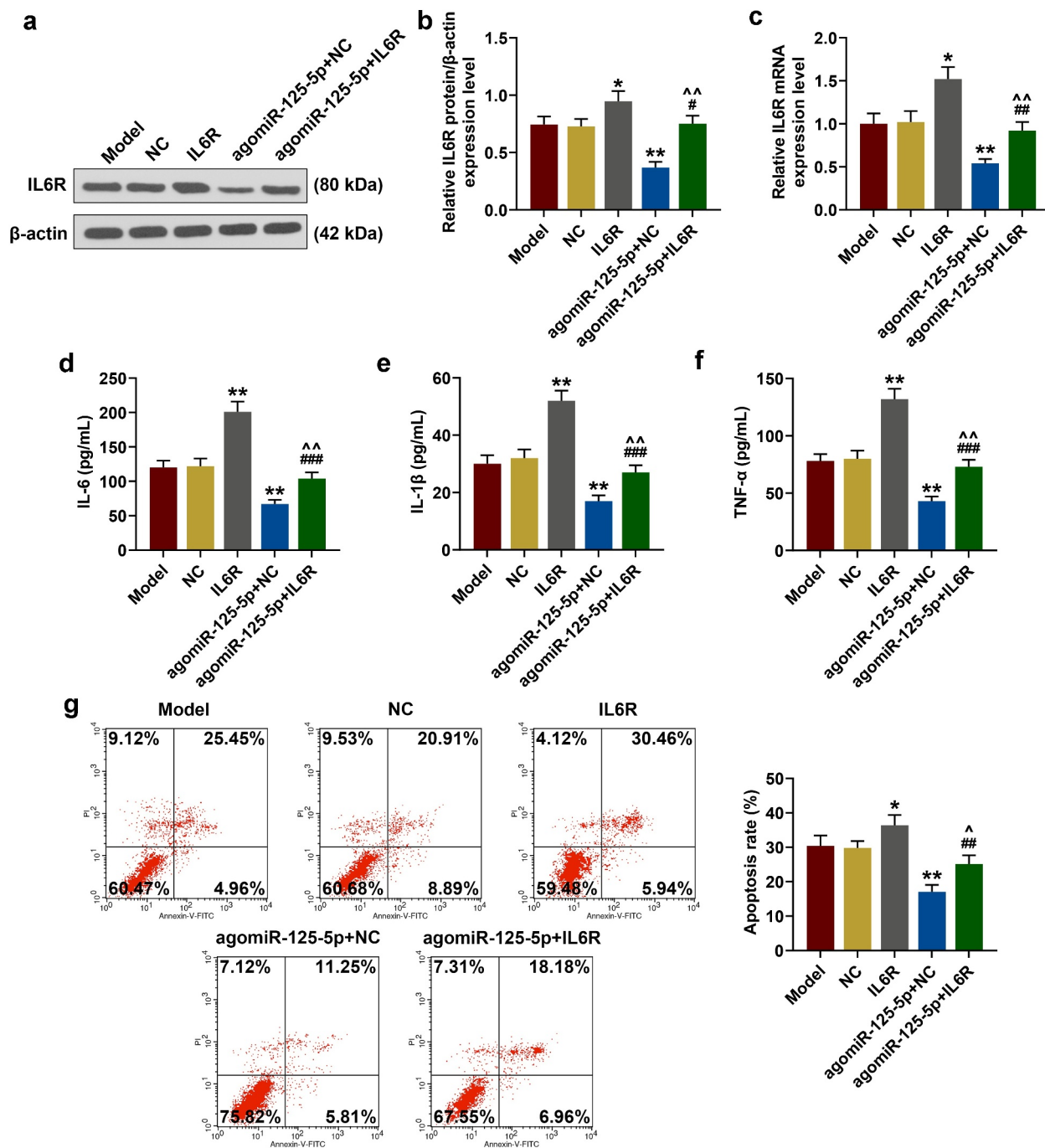


Figure 4. Effect of IL-6 R overexpression on co-culture system of monocyte cells (THP-1) and human intestinal epithelial cells (NCM460). (a-c) After co-culture of THP-1 and NCM460 for 24 hours, the expression of IL-6 R in THP-1 cells of Model, NC, IL-6 R, agomiR-125-5p+NC, agomiR-125-5p+IL6 R group was detected by reverse transcription quantitative polymerase chain reaction (RT-qPCR) and Western blot. (d-f) Enzyme-linked immunosorbent assay (ELISA) was used to determine the contents of interleukin-6 (IL-6), IL-1β and tumor necrosis factor-α (TNF-α) in the supernatant of medium in each group. (g) After 24-h co-culture of THP-1 and NCM460, the apoptosis of NCM460 cells in each group was detected by flow cytometry. All the experiments have been performed in triplicate. β-actin was used as a control. * $P < 0.05$, ** $P < 0.01$ vs. NC; # $P < 0.05$, ## $P < 0.01$, ### $P < 0.001$ vs. IL-6 R; ^ $P < 0.05$, ^^ $P < 0.01$ vs. agomiR-125-5p+NC.

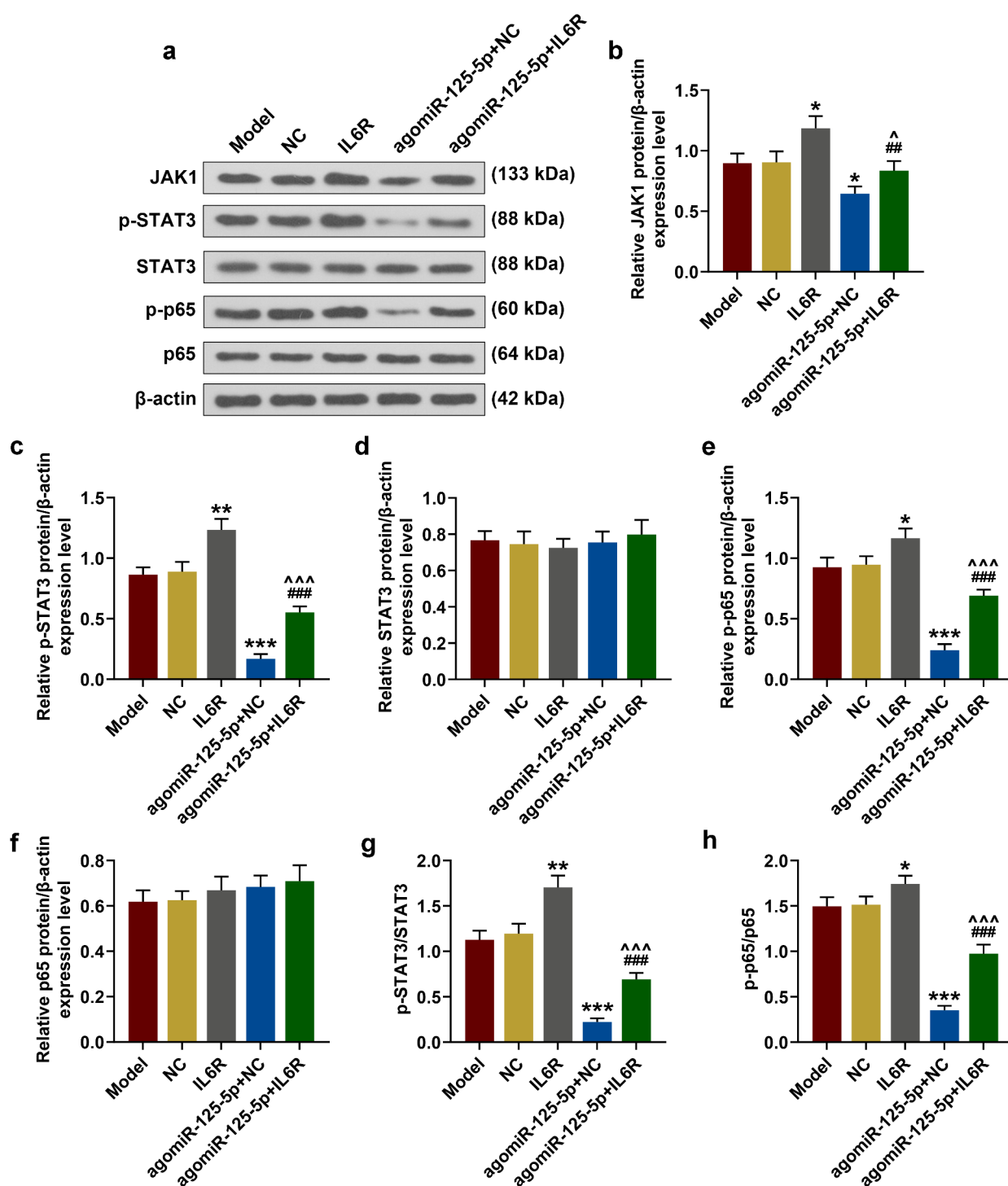


Figure 5. (a-h) Western blot was used to detect the expressions of JAK1, p-STAT3, STAT3, p-p65 and p65 in the Model, NC, IL-6 R, agomiR-125-5p + NC, agomiR-125-5p + IL-6 R group. All the experiments have been performed in triplicate. β-actin was used as a control. * $P < 0.05$, ** $P < 0.01$, *** $P < 0.001$ vs. NC; # $P < 0.01$, ### $P < 0.001$ vs. IL-6 R; ^ $P < 0.05$, ^^^ $P < 0.001$ vs. agomiR-125-5p + NC.

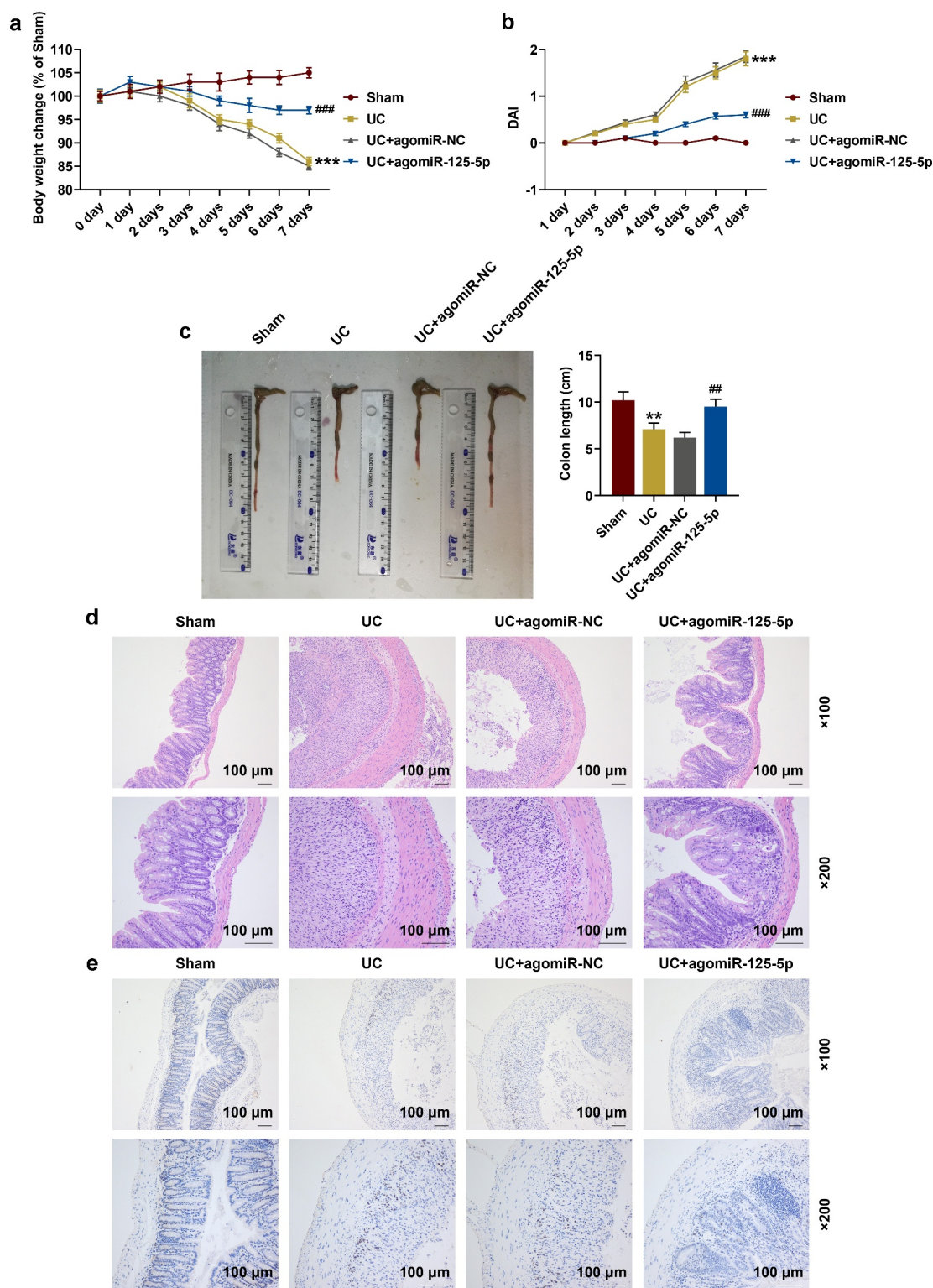


Figure 6. Effects of miR-125-5p agomiR on body weight, DAI, colon length, histopathological changes, and apoptosis in ulcerative colitis (UC) mouse models. (a) Changes in body weight of mice in the Sham, UC, UC + agomiR-NC, and UC + agomiR-125-5 groups were recorded. (b) The disease activity index (DAI) of each group of mice was scored according to the average value of the three parameters of stool consistency, stool blood and percent weight loss. (c) Colonic length of the mice in each group was measured. (d) Histopathological changes in the colon of mice in each group were evaluated using hematoxylin-eosin (H&E) staining. Scale = 100 μm. (e) Apoptosis levels in colon tissues of mice in each group were measured by TUNEL method. Scale = 100 μm. All the experiments have been performed triplicate. ** $P < 0.01$, *** $P < 0.001$ vs. Sham; ## $P < 0.01$, ### $P < 0.001$ vs. UC + agomiR-NC.

miR-125-5p agomiR affected UC mouse models through IL-6 R *in vivo*

In order to further clarify whether IL-6 R and miR-125-5p had the same regulatory effects *in vivo*, the expression of miR-125-5p in the colon tissues of the mice in each group was determined. As shown in Figure 7(d), as compared with the Sham group, the expression of miR-125-5p in the colon tissues of the mice in the UC group was significantly reduced, which, however, was greatly

increased by agomiR-125-5p injection ($P < 0.001$). The data also revealed that the expression of IL-6 R in the colon tissues of the mice in UC group was significantly higher than that in Sham group, and agomiR-125-5p injection noticeably reduced the expression of IL-6 R (Figure 7(e)). As expected, the results obtained here supported those of Western blot ($P < 0.01$, Figure 8(a-i)). We also found that compared with the Sham group, the expression of JAK1 and the levels of STAT3 and

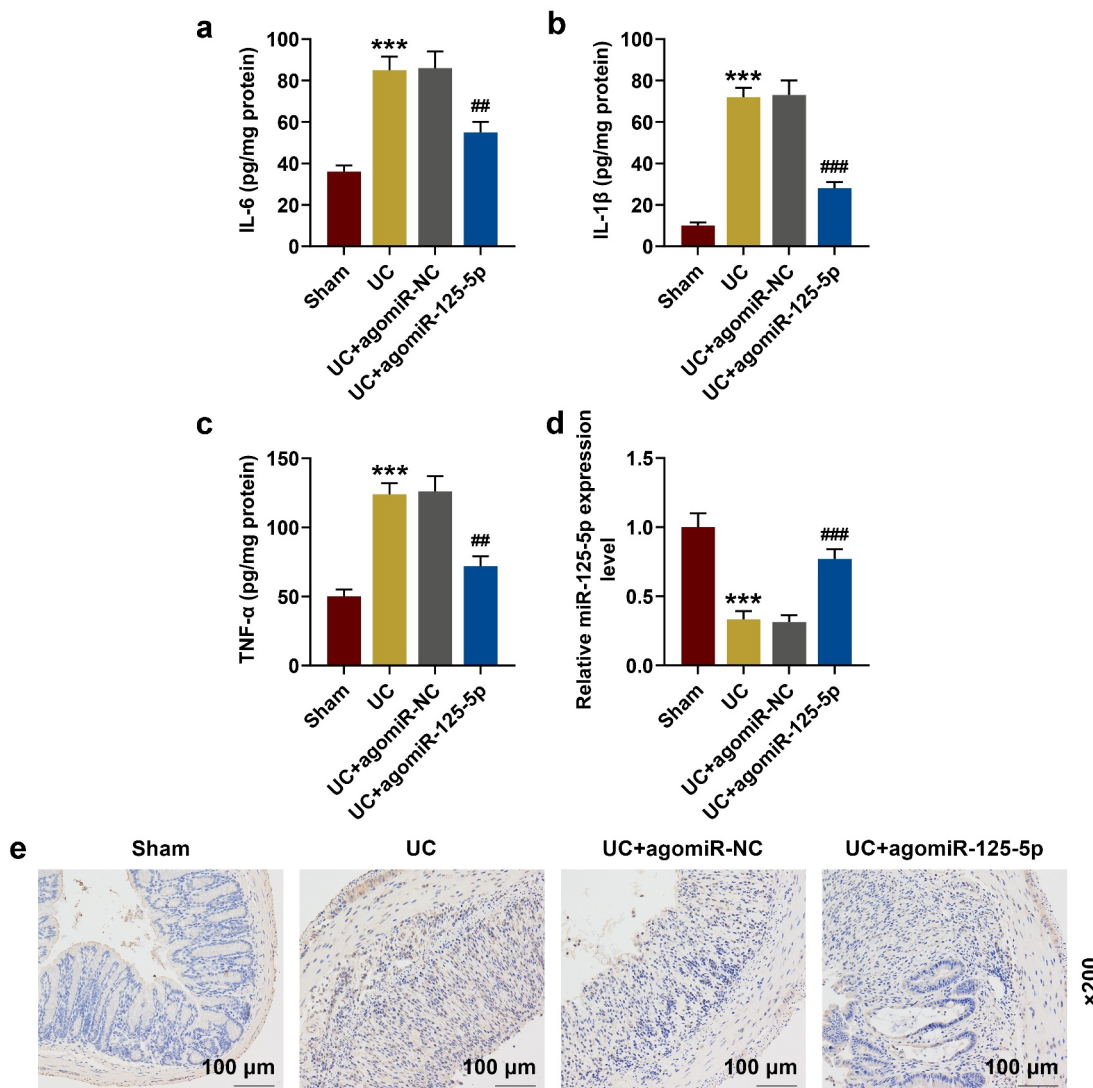


Figure 7. MiR-125-5p agomiR affects the expression of inflammatory factors, miR-125-5p and IL-6 R in ulcerative colitis (UC) mouse model. (a-c) The expression of interleukin-6 (IL-6), IL-1 β and tumor necrosis factor- α (TNF- α) in the colon tissue homogenates of mice in the Sham, UC, UC + agomiR-NC, and UC + agomiR-125-5 groups was measured using enzyme-linked immunosorbent assay (ELISA). (d) The expression of miR-125-5p in the colon tissues of each group of mice was detected by reverse transcription real-time quantitative polymerase chain reaction (RT-qPCR). (e) The expression of IL-6 R in colon tissues of mice in each group was detected by immunohistochemistry. Magnification $\times 200$, Scale = 100 μm . All experiments have been performed in triplicate. *** $P < 0.001$ vs. Sham; ## $P < 0.01$, ### $P < 0.001$ vs. UC + agomiR-NC.

p65 phosphorylation were significantly increased in the UC group, and agomiR-125-5p injection could greatly reverse the activation of JAK1/STAT3 and NF- κ B pathways in the UC group. In addition, we found that compared with overexpression of miR-125-5p, IL-6 R silencing can also

achieve the same effect of improving UC as overexpression of miR-125-5p did. Immunofluorescence detection of p65 metastasis showed that the p65 content in the nucleus of the UC and UC+agomiR-NC groups was increased significantly, and that the overexpression of miR-

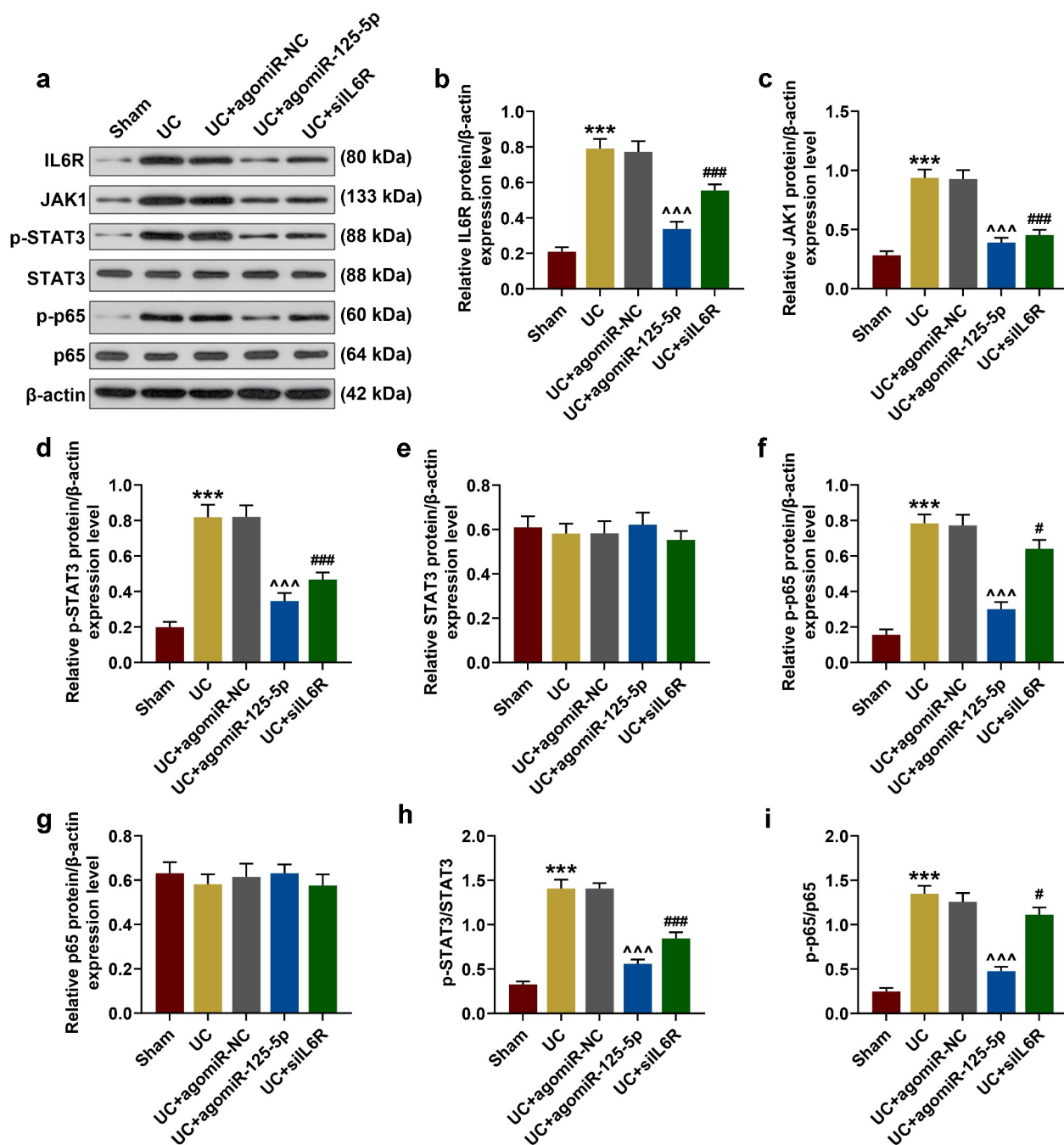


Figure 8. (a-i) Western blot was used to detect the expressions of IL-6 R, JAK1, p-STAT3, STAT3, p-p65 and p65 in colon tissues of mice in Sham, UC, UC + agomiR-NC, UC + agomiR-125-5 and UC + siIL6R groups. All the experiments have been performed in triplicate. *** $P < 0.001$ vs. Sham; # $P < 0.05$, ## $P < 0.01$, ### $P < 0.001$ vs. UC; ^^^ $P < 0.001$ vs. UC + agomiR-NC.

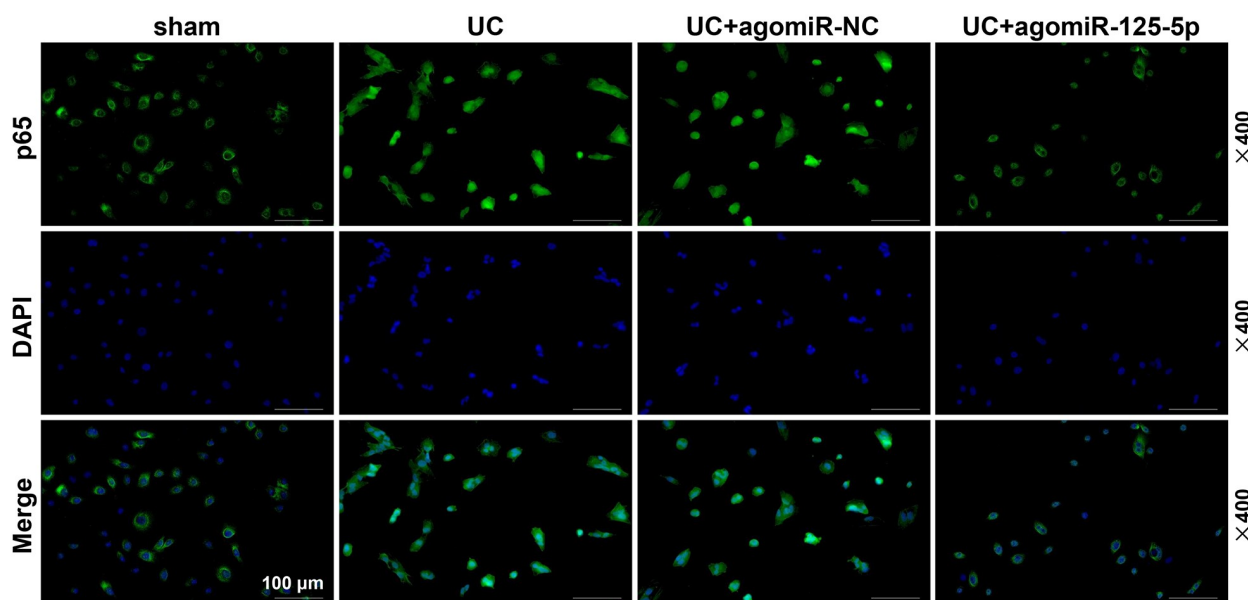


Figure 9. Fluorescence microscopy (BX61, Olympus, Japan) was used to observe the transfer of p65 in mouse intestinal epithelial cell nucleus. We found that within 1 h of staining, p65 translocation was found in the UC group and the UC+ agomiR-NC group.

125-5p could sharply reduce the nuclear content of p65 (Figure 9).

Discussion

The current study found that IL-6 R was abnormally high-expressed and miR-125-5p was low-expressed in the serum specimens of UC patients. Exosomes are important vectors for miRNA transport, and studies have increasingly found that miRNAs derived from exosomes play an important regulatory role in biological functions [25,26]. Therefore, we speculated that the source of miR-125-5p in the serum of UC patients might be from exosomes. Further investigation revealed that IL-6 R expression can be inhibited by specific targeted binding of miR-125-5p. In *in vitro* experiment, we established an acute conjunctivitis cell model, and observed that IL-6 R overexpression was associated with inflammatory release in macrophages and increased apoptosis of intestinal epithelial cells, but miR-125-5p up-regulation partially reversed the role of IL-6 R. In *in vivo* experiments, we found that miR-125-5p up-regulation significantly increase body weight and colon length, and greatly reduced the infiltration of inflammatory cells and the production of pro-inflammatory

mediators in the serum and colon. At the same time, the above changes were accompanied by reduced expression of IL-6 R and inhibition of JAK1/STAT3 and NF- κ B pathway activation.

A large number of basic and clinical studies have shown that under the influence of environmental factors, genetically susceptible patients could develop abnormal intestinal immune response, which will cause abnormal activation of immune cell dysfunction, ultimately leading to the incidence of UC, and that the intestinal mucosal immune homeostasis is the direct cause of UC [19,27]. Studies increasingly demonstrated that anti-inflammatory and regulating immune response can effectively improve the excessive immune and inflammatory response in UC patients [28]. Previously, it has been found that IL-6 R is high-expressed in UC patients [18], which was also verified in our experiments, because we also observed that IL-6 R may play a pro-inflammatory role in UC. At present, it has been widely acknowledged that miRNAs targeting the transcription of proteins to encode the intestinal barrier and its receptors [29]. miRNAs can affect the secretion of downstream inflammatory factors or participate in the development and differentiation of the immune system through

specific interaction with target gene sequences, thus participating in the occurrence and development of chronic inflammatory responses [30]. Our study showed that miR-125-5p expression was reduced in UC patients, which was consistent with the findings from previous studies. However, past research did not examine the role and mechanism of miR-125-5p and IL-6 R in UC [18]. We found that miR-125-5p and IL-6 R were negatively correlated and there was a target binding relationship between the two, indicating that miR-125-5p may inhibit the inflammatory response through inhibiting IL-6 R expression.

Study discovered abnormal expression profiles of miRNAs in a variety of diseases, including in UC [9]. The abnormal expression of miRNA in UC cells can suppress or activate the expressions of target genes [7,31]. Our results indicated that miR-125-5p overexpression inhibited the expression of IL-6 R in UC. It has been found that up-regulation of miR-21 expression causes Rho-mRNA degradation to increase intestinal epithelial permeability, disrupt the intestinal mucosal barrier, and increase inflammation [32]. Cytokines play an important role in mediating and regulating immune and inflammatory responses, and are closely related to the pathogenesis of UC [4]. The imbalance between the pro-inflammatory cytokine and anti-inflammatory cytokine is considered to be a crucial factor leading to the pathogenesis of UC [27]. Researchers observed that NF- κ B is the “master switch” for the expressions of various proinflammatory mediator genes [33]. In addition, the JAK1/STAT3 pathway is an important signaling pathway regulating biological behaviors such as cell growth, apoptosis, differentiation, and migration. In cell apoptosis, mitochondrial pathway apoptosis is a critical biological process regulated by the JAK1/STAT3 signaling pathway [34]. We found that in UC cell models, up-regulating miR-125-5p expression inhibited the inflammatory response and activation of JAK1/STAT3 and NF- κ B pathways, reduced the apoptosis of intestinal epithelial cells, but overexpression of IL-6 R can partially reverse the effect of miR-125-5p, suggesting that miR-125-5p targeting IL-6 R improved inflammatory response and over-immunity in the UC cell model.

Parallel experiments *in vivo* have been previously performed. Studies found that miR-19a expression was significantly reduced and TNF- α expression was greatly increased in DSS-treated mouse colitis and in colon tissue of UC patients [35]. In this study, we also used the DSS-induced UC mouse model for investigation. Interestingly, miR-125-5p overexpression was found to noticeably ameliorate the severity of colitis in the mice in the UC group, which was supported by reduced DAI score, tissue damage, apoptosis, and inflammatory response. It should be noted that miR-125-5p up-regulation significantly reduced the expression of IL-6 R in the UC mice and the expression of JAK1, STAT3 and p65 phosphorylation in colon tissues of the UC mice.

In conclusion, the current study was the first to report that miR-125-5p targeting IL-6 R inhibits inflammatory response in UC and reduces the apoptosis of intestinal epithelial cells, and such a mechanism may contribute to the pathological development of UC through JAK1/STAT3 and NF- κ B pathways. However, at present, the sample size of patients in our study was small, which therefore requires future study in depth. Funding This work is supported by Natural Science Foundation of Shanghai (19ZR1429700), National Natural Science Foundation of China (81802303), Research Project of Pudong New Area Health and Family Planning Commission (PW2018D-01), and Clinical Research Program of Shanghai Ninth People’s Hospital (JYLJ022).

Availability of Data and Materials

The analyzed data sets generated during the study are available from the corresponding author on reasonable request.

Disclosure statement

No potential conflict of interest was reported by the author (s).

References

- [1] Hodson R. Inflammatory bowel disease. *Nature*. 2016 Dec 21;540(7634):S97. PubMed PMID: 28002398.

- [2] Sachar DB. Ulcerative colitis: dead or alive. *Ann Intern Med.* **2015** Aug 18;163(4):316–317. PubMed PMID: 26167671.
- [3] Buch KE. Inflammatory bowel disease. A clinical review of Crohn's disease and ulcerative colitis. *Adv Nurse Pract.* **2007** Jul;15(7):57–60. PubMed PMID: 19998998.
- [4] Guan Q, Zhang J. Recent advances: the imbalance of cytokines in the pathogenesis of inflammatory bowel disease. *Mediators Inflamm.* **2017**;2017:4810258. PubMed PMID: 28420941; PubMed Central PMCID: PMC5379128.
- [5] Beerhmann J, Piccoli MT, Viereck J, et al. Non-coding RNAs in development and disease: background, mechanisms, and therapeutic approaches. *Physiol Rev.* **2016** Oct;96(4):1297–1325. PubMed PMID: 27535639.
- [6] Sanjay S, Girish C. Role of miRNA and its potential as a novel diagnostic biomarker in drug-induced liver injury. *Eur J Clin Pharmacol.* **2017** Apr;73(4):399–407. PubMed PMID: 28028586.
- [7] Viennois E, Zhao Y, Han MK, et al. Serum miRNA signature diagnoses and discriminates murine colitis subtypes and predicts ulcerative colitis in humans. *Sci Rep.* **2017** May 31;7(1):2520. PubMed PMID: 28566745; PubMed Central PMCID: PMC5451415.
- [8] Benderska N, Dittrich AL, Knaup S, et al. miRNA-26b Overexpression in Ulcerative Colitis-associated Carcinogenesis. *Inflamm Bowel Dis.* **2015** Sep;21(9):2039–2051. PubMed PMID: 26083618; PubMed Central PMCID: PMC4603667.
- [9] Netz U, Carter J, Eichenberger MR, et al. Plasma microRNA profile differentiates crohn's colitis from ulcerative colitis. *Inflamm Bowel Dis.* **2017** Dec 19;24(1):159–165. PubMed PMID: 29272478; PubMed Central PMCID: PMC5858028.
- [10] Cai M, Chen S, Hu W. MicroRNA-141 is involved in ulcerative colitis pathogenesis via aiming at CXCL5. *J Interferon Cytokine Res.* **2017** Sep;37(9):415–420. PubMed PMID: 28854064.
- [11] He C, Yu T, Shi Y, et al. MicroRNA 301A promotes intestinal inflammation and colitis-associated cancer development by inhibiting BTG1. *Gastroenterology.* **2017** May;152(6):1434–1448e15. PubMed PMID: 28193514.
- [12] Cordes F, Bruckner M, Lenz P, et al. MicroRNA-320a strengthens intestinal barrier function and follows the course of experimental colitis. *Inflamm Bowel Dis.* **2016** Oct;22(10):2341–2355. PubMed PMID: 27607334.
- [13] Koukos G, Polyarchou C, Kaplan JL, et al. MicroRNA-124 regulates STAT3 expression and is down-regulated in colon tissues of pediatric patients with ulcerative colitis. *Gastroenterology.* **2013** Oct;145(4):842–52e2. PubMed PMID: 23856509; PubMed Central PMCID: PMC4427058.
- [14] Wolf J, Rose-John S, Garbers C. Interleukin-6 and its receptors: a highly regulated and dynamic system. *Cytokine.* **2014** Nov;70(1):11–20. PubMed PMID: 24986424.
- [15] Jordan SC, Choi J, Kim I, et al. Interleukin-6, A cytokine critical to mediation of inflammation, autoimmunity and allograft rejection: therapeutic implications of IL-6 receptor blockade. *Transplantation.* **2017** Jan;101(1):32–44. PubMed PMID: 27547870.
- [16] Schmidt-Arras D, Rose-John S. IL-6 pathway in the liver: from physiopathology to therapy. *J Hepatol.* **2016** Jun;64(6):1403–1415. PubMed PMID: 26867490.
- [17] Leu CM, Wong FH, Chang C, et al. Interleukin-6 acts as an antiapoptotic factor in human esophageal carcinoma cells through the activation of both STAT3 and mitogen-activated protein kinase pathways. *Oncogene.* **2003** Oct 30;22(49):7809–7818. PubMed PMID: 14586407.
- [18] Parisinos CA, Serghiou S, Katsoulis M, et al. Variation in interleukin 6 receptor gene associates with risk of crohn's disease and ulcerative colitis. *Gastroenterology.* **2018** Aug;155(2):303–306e2. PubMed PMID: 29775600; PubMed Central PMCID: PMC6083435.
- [19] Tatiya-Aphiradee N, Chatuphonprasert W, Jarukamjorn K. Immune response and inflammatory pathway of ulcerative colitis. *J Basic Clin Physiol Pharmacol.* **2018** Dec 19;30(1):1–10. PubMed PMID: 30063466.
- [20] Lu X, Yu Y, Tan S. The role of the miR-21-5p-mediated inflammatory pathway in ulcerative colitis. *Exp Ther Med.* **2020** Feb;19(2):981–989. PubMed PMID: 32010260; PubMed Central PMCID: PMC6966149.
- [21] Li M, Zhang S, Qiu Y, et al. Upregulation of miR-665 promotes apoptosis and colitis in inflammatory bowel disease by repressing the endoplasmic reticulum stress components XBP1 and ORMDL3. *Cell Death Dis.* **2017** Mar 23;8(3):e2699. PubMed PMID: 28333149; PubMed Central PMCID: PMC5386569.
- [22] Singh C, Roy-Chowdhuri S. Quantitative real-time PCR: recent advances. *Methods Mol Biol.* **2016**;1392:161–176. PubMed PMID: 26843055.
- [23] Chen Y, Le TH, Du Q, et al. Genistein protects against DSS-induced colitis by inhibiting NLRP3 inflammasome via TGR5-cAMP signaling. *Int Immunopharmacol.* **2019** Jun;71:144–154. PubMed PMID: 30901677.
- [24] Ren MT, Gu ML, Zhou XX, et al. Sirtuin 1 alleviates endoplasmic reticulum stress-mediated apoptosis of intestinal epithelial cells in ulcerative colitis. *World J Gastroenterol.* **2019** Oct 14;25(38):5800–5813. PubMed PMID: 31636473; PubMed Central PMCID: PMC6801188.

- [25] Yu X, Odenthal M, Fries JW. Exosomes as miRNA carriers: formation-function-future. *Int J Mol Sci.* 2016 Dec 2. 17(12). PubMed PMID: 27918449; PubMed Central PMCID: PMC5187828. eng. DOI: [10.3390/ijms17122028](https://doi.org/10.3390/ijms17122028)
- [26] Xie Y, Chen Y, Zhang L, et al. The roles of bone-derived exosomes and exosomal microRNAs in regulating bone remodelling. *J Cell Mol Med.* 2017 May;21(5):1033–1041. PubMed PMID: 27878944; PubMed Central PMCID: PMC5387131. eng.
- [27] Ordas I, Eckmann L, Talamini M, et al. Ulcerative colitis. *Lancet.* 2012 Nov 3;380(9853):1606–1619. PubMed PMID: 22914296.
- [28] Shen ZH, Zhu CX, Quan YS, et al. Relationship between intestinal microbiota and ulcerative colitis: mechanisms and clinical application of probiotics and fecal microbiota transplantation. *World J Gastroenterol.* 2018 Jan 7;24(1):5–14. PubMed PMID: 29358877; PubMed Central PMCID: PMC5757125.
- [29] Soroosh A, Rankin CR, Polytarchou C, et al. miR-24 is elevated in ulcerative colitis patients and regulates intestinal epithelial barrier function. *Am J Pathol.* 2019 Sep;189(9):1763–1774. PubMed PMID: 31220450; PubMed Central PMCID: PMC6723227.
- [30] Deng F, He S, Cui S, et al. A molecular targeted immunotherapeutic strategy for ulcerative colitis via dual-targeting nanoparticles delivering miR-146b to intestinal macrophages. *J Crohns Colitis.* 2019 Mar 30;13(4):482–494. PubMed PMID: 30445446.
- [31] Deng S, Wang H, Fan H, et al. Over-expressed miRNA-200b ameliorates ulcerative colitis-related colorectal cancer in mice through orchestrating epithelial-mesenchymal transition and inflammatory responses by channel of AKT2. *Int Immunopharmacol.* 2018 Aug;61:346–354. PubMed PMID: 29933193.
- [32] Yang Y, Ma Y, Shi C, et al. Overexpression of miR-21 in patients with ulcerative colitis impairs intestinal epithelial barrier function through targeting the Rho GTPase RhoB. *Biochem Biophys Res Commun.* 2013 May 17;434(4):746–752. PubMed PMID: 23583411.
- [33] Ma J, Yin G, Lu Z, et al. Casticin prevents DSS induced ulcerative colitis in mice through inhibitions of NF-kappaB pathway and ROS signaling. *Phytother Res.* 2018 Sep;32(9):1770–1783. PubMed PMID: 29876982.
- [34] Chu XQ, Wang J, Chen GX, et al. Overexpression of microRNA-495 improves the intestinal mucosal barrier function by targeting STAT3 via inhibition of the JAK/STAT3 signaling pathway in a mouse model of ulcerative colitis. *Pathol Res Pract.* 2018 Jan;214(1):151–162. PubMed PMID: 29129493.
- [35] Chen B, She S, Li D, et al. Role of miR-19a targeting TNF-alpha in mediating ulcerative colitis. *Scand J Gastroenterol.* 2013 Jul;48(7):815–824. PubMed PMID: 23795660.